

Bounds on Heavy-to-Heavy Baryonic Form Factors

Cheng-Wei Chiang*

Department of Physics, Carnegie Mellon University, Pittsburgh, PA 15213

Abstract

Upper and lower bounds are established on the $\Lambda_b \rightarrow \Lambda_c$ semileptonic decay form factors by utilizing inclusive heavy-quark-effective-theory sum rules. These bounds are calculated to leading order in Λ_{QCD}/m_Q and α_s . The $O(\alpha_s^2 \beta_0)$ corrections to the bounds at zero recoil are also presented. Several form factor models used in the literature are compared with our bounds.

*chengwei@andrew.cmu.edu

I. INTRODUCTION

In the early development of heavy quark physics, much attention were put on the semileptonic heavy meson decays $B \rightarrow D^{(*)}l\bar{\nu}$ in order to extract information about the Kobayashi-Maskawa matrix element $|V_{cb}|$ [1]. As more and more data will accumulate for semileptonic heavy baryon decays, they can also serve as another independent determination of $|V_{cb}|$ [2–4].

We have recently performed a thorough analysis of the bounds on the $B \rightarrow D^{(*)}$ weak decay form factors using inclusive sum rules for semileptonic decays to order Λ_{QCD}/m_Q and first order in α_s [5]. The $\mathcal{O}(\alpha_s^2\beta_0)$ corrections at zero recoil were also included. In the present paper, we would like to extend the techniques in our previous work to baryons that contain a heavy quark.

As in the case of heavy mesons, heavy-to-heavy baryonic form factors are mainly taken from models. They are extensively used in the studies of backgrounds and efficiencies in experiments, and, for this reason alone, constraining them is important. For $\Lambda_b \rightarrow \Lambda_c$ transitions, where the initial and final baryons have the same light degrees of freedom, the Heavy Quark Effective Theory (HQET) relates all six form factors to a single Isgur-Wise function and predicts a specific value at zero recoil in the infinite mass limit [6]. In the HQET, the form factors and Isgur-Wise function are usually written as functions of $\omega = v \cdot v'$, with v being the four-velocity of the Λ_b baryon and v' that of the recoiling Λ_c baryon.

The analysis for heavy baryons is almost parallel to that for heavy mesons. One difference is the HQET parameters and heavy hadron masses appearing in each case. Another difference is that heavy baryons have an extra light quark. However, we will see that the power of inclusive sum rules still applies, regardless of the intricacy among the light degrees of freedom.

The layout of this paper is as follows: In Section II, we list the sum rule formulae for the model-independent bounds on form factors defined in Section III. Section III also gives the proper combinations of structure functions used later for the bounds on each of the baryonic

form factors. Section IV provides the bounds on individual form factors explicitly, with the structure functions given in [5], and discusses the influence of the various parameters appearing in the expansion of the bounds. Some popular form factor models are compared with our bounds in Section V. Order $\alpha_S^2 \beta_0$ corrections to the bounds at zero recoil are computed in Section VI. In Section VII, the bounds on the $\Lambda_b \rightarrow \Lambda_c l \nu$ decay spectrum and the slope are given. Our conclusions are summarized in Section VIII.

II. INCLUSIVE HQET SUM RULES

The sum rules are obtained by relating the inclusive decay rate, calculated using the operator product expansion (OPE) and perturbative QCD in the partonic picture, to the sum of exclusive decays rates, calculated in the hadronic picture. Since these had been derived previously [7–9,5], we just write down the results below. The same formalism can be applied to all types of heavy baryons. Nevertheless, we will concentrate exclusively on Λ -type ground-state baryons and denote them by Λ_Q .

Let $|\Lambda_Q(v, s)\rangle$ be the state of the heavy baryon Λ_Q with mass M_{Λ_Q} and spin s moving with four-velocity v and $|\Lambda_{Q'}(v', s')\rangle$ that of the Λ'_Q with energy $E_{\Lambda_{Q'}}$ and spin s' moving with four-velocity v' . $E_{\Lambda_{Q'}} = \sqrt{M_{\Lambda_{Q'}}^2 + q_3^2}$, where q_3 is the z component of the momentum transfer, q , to the leptonic sector and \vec{q} is pointing in the z direction. Consider the time ordered product of two weak transition currents between Λ_Q baryons in momentum space,

$$\begin{aligned} T^{\mu\nu} &= \frac{i}{2M_{\Lambda_Q}} \frac{1}{2j+1} \sum_s \int d^4x e^{-iq \cdot x} \langle \Lambda_Q(v, s) | T(J^{\mu\dagger}(x) J^\nu(0)) | \Lambda_Q(v, s) \rangle \\ &= -g^{\mu\nu} T_1 + v^\mu v^\nu T_2 + i\epsilon^{\mu\nu\alpha\beta} q_\alpha v_\beta T_3 + q^\mu q^\nu T_4 + (q^\mu v^\nu + v^\mu q^\nu) T_5, \end{aligned} \quad (1)$$

where J^μ is a $Q \rightarrow Q'$ axial or vector current and j is the spin of $|\Lambda_Q(v, s)\rangle$. The bounds are then

$$\begin{aligned} \frac{1}{2\pi i} \int_C d\epsilon \theta(\Delta - \epsilon) T(\epsilon) \left(1 - \frac{\epsilon}{E_1 - E_{\Lambda_{Q'}}} \right) &\leq \frac{M_{\Lambda_{Q'}}}{2j+1} \sum_{s, s'} \frac{|\langle \Lambda_{Q'}(v', s') | a \cdot J | \Lambda_Q(v, s) \rangle|^2}{4M_{\Lambda_Q} E_{\Lambda_{Q'}}} \\ &\leq \frac{1}{2\pi i} \int_C d\epsilon \theta(\Delta - \epsilon) T(\epsilon), \end{aligned} \quad (2)$$

where $T(\epsilon) \equiv a_\mu^* T^{\mu\nu} a_\nu$, the product of $T^{\mu\nu}$ and four-vectors $a_\mu^* a_\nu$. The integration variable $\epsilon = M_{\Lambda_Q} - E_{\Lambda_{Q'}} - v \cdot q$, E_1 is the energy of the first excited state more massive than $\Lambda_{Q'}$, and Δ is the scale up to which the perturbation sums over.

The upper bound is essentially model independent, while the lower bound relies on the assumption that there is no multiparticle production of hadrons in the final state. This additional assumption is in accord with the large N_c limit and is supported as well by current experimental results. These bounds can be used for the decays at arbitrary momentum transfer q^2 . Since $1/(E_1 - E_{\Lambda_{Q'}}) \sim 1/\Lambda_{\text{QCD}}$, the lower bounds will be limited to first order in $1/m_Q$. The upper bounds, on the other hand, can be calculated to order $1/m_Q^2$ without additional HQET parameters.

The above formulae are presented in terms of Λ -type baryons, however, they can be readily applied to other types of baryons too. Later on, we will restrict our analysis exclusively to the Λ -type semileptonic decays with $Q \rightarrow b$ and $Q' \rightarrow c$, *i.e.*, the $\Lambda_b \rightarrow \Lambda_c l \bar{\nu}$ decays for which $j = 1/2$.

III. HADRONIC SIDE

The hadronic matrix elements for semileptonic decays of a Λ_b baryon into a Λ_c baryon are conventionally parameterized in terms of six form factors defined by

$$\begin{aligned} \langle \Lambda_c(v', s') | V^\mu | \Lambda_b(v, s) \rangle &= \bar{u}_{\Lambda_c}(v', s') \left[F_1(\omega) \gamma^\mu + F_2(\omega) v^\mu + F_3(\omega) v'^\mu \right] u_{\Lambda_b}(v, s), \\ \langle \Lambda_c(v', s') | A^\mu | \Lambda_b(v, s) \rangle &= \bar{u}_{\Lambda_c}(v', s') \left[G_1(\omega) \gamma^\mu + G_2(\omega) v^\mu + G_3(\omega) v'^\mu \right] \gamma_5 u_{\Lambda_b}(v, s). \end{aligned} \quad (3)$$

One may relate the parameter ω to the momentum transfer q^2 by $\omega = (M_{\Lambda_b}^2 + M_{\Lambda_c}^2 - q^2)/(2M_{\Lambda_b}M_{\Lambda_c})$. With proper choices of the current J^μ and the four-vector a_μ , one can readily select the form factor of interest and, from Eq. (2), form the corresponding bounds. To subleading order in $1/m_Q$ in HQET, these form factors satisfy the relations: [10,11]

$$F_1 = \zeta(\omega) \left[1 + \bar{\Lambda} \left(\frac{1}{2m_c} + \frac{1}{2m_b} \right) \right], \quad (4)$$

$$\begin{aligned}
G_1 &= \zeta(\omega) \left[1 + \bar{\Lambda} \left(\frac{1}{2m_c} + \frac{1}{2m_b} \right) \frac{\omega - 1}{\omega + 1} \right], \\
F_2(\omega) &= G_2(\omega) = -\frac{\bar{\Lambda}}{m_c} \frac{1}{\omega + 1} \zeta(\omega), \\
F_3(\omega) &= -G_3(\omega) = -\frac{\bar{\Lambda}}{m_b} \frac{1}{\omega + 1} \zeta(\omega).
\end{aligned}$$

In the above equations, we have absorbed the corrections from the subleading kinematic energy into the Isgur-Wise function, $\zeta(\omega)$.

To bound F_1 (or G_1), one may choose $J^\mu = V^\mu$ (or A^μ) and $a^\mu = (0, 1, 0, 0)$. Then the factor to be bounded is $\frac{(\omega-1)}{2\omega} |F_1(\omega)|^2 \left(\frac{\omega+1}{2\omega} |G_1(\omega)|^2 \right)$ and the sum rule used to bound is $T_{1OPE} = T_{1Hadronic}$. In this and the following cases, the corresponding first excited state more massive than Λ_c that contributes to the sum rule is the $\Lambda_c(2593)$ state.¹

It is impossible to bound F_2 and F_3 individually with any choice of a^μ . The next best thing we can do is to bound a linear combination of them. To prevent the bounds from diverging at zero recoil, we choose $J^\mu = V^\mu$ and $a^\mu = (\sqrt{E_{\Lambda_c}/M_{\Lambda_c} - 1}, 0, 0, -\sqrt{E_{\Lambda_c}/M_{\Lambda_c} - 1})$. Then the factor to be bounded is $\frac{\omega^2-1}{2\omega} |F_2 - F_3|^2$, and the sum rule requires the following combination of structure functions

$$\begin{aligned}
T(\epsilon) &= 2T_1 + (\omega - 1)T_2 + (M_{\Lambda_b} + M_{\Lambda_c} - \epsilon)^2 (\omega - 1)T_4 \\
&\quad + 2(M_{\Lambda_b} + M_{\Lambda_c} - \epsilon)(\omega - 1)T_5.
\end{aligned} \tag{5}$$

A similar situation occurs for G_2 and G_3 . Here the choice would be $J^\mu = A^\mu$ and $a^\mu = (1, 0, 0, -\sqrt{\frac{E_{\Lambda_c}-M_{\Lambda_c}}{E_{\Lambda_c}+M_{\Lambda_c}}})$. The bounded factor is $\frac{\omega-1}{2\omega} |G_2 + G_3|^2$, and

$$\begin{aligned}
T(\epsilon) &= -\frac{2}{\omega + 1} T_1 + T_2 + (M_{\Lambda_b} - M_{\Lambda_c} - \epsilon)^2 T_4 \\
&\quad + 2(M_{\Lambda_b} - M_{\Lambda_c} - \epsilon) T_5
\end{aligned} \tag{6}$$

is the combination for the sum rule.

From Eq. (4), we know $|F_2 - F_3|^2 = |G_2 + G_3|^2 \sim 1/m_Q^2$ at this order in HQET.

¹ $\Sigma_c(2455)$ is lighter, but $\Lambda_b \rightarrow \Sigma_c(2455)l\nu$ is not an allowed transition because of the isospin.

IV. PARTONIC SIDE AND THE BOUNDS

The analysis will be performed to first order in $\alpha_s(m_Q)$ (~ 0.3 at 2 GeV) and Λ_{QCD}/m_Q and, furthermore, only terms linear in $\omega - 1$ are kept for the perturbative part. The full ω dependence will be kept in the nonperturbative physics. Corrections of order $\Lambda_{\text{QCD}}^2/m_Q^2$, α_s^2 , $\alpha_s \Lambda_{\text{QCD}}/m_Q$, and $\alpha_s (\omega - 1)^2$ should be negligible in the kinematic region that we are considering.

We will use essentially the same notation as in [5]. Since Λ_b and Λ_c are spin- $\frac{1}{2}$ baryons where the light degrees of freedom carry zero angular momentum, the chromomagnetic energy $\lambda_2 = 0$. Also, the heavy quark parameters $\bar{\Lambda}$ and λ_1 for the baryons are different from those for the mesons. Their values, however, can be obtained from those of mesons by the two relations [12]

$$\begin{aligned}\bar{\Lambda}^B &= \bar{\Lambda}^M + \frac{m_b}{m_b - m_c} (M_{\Lambda_b} - \bar{M}_B) - \frac{m_c}{m_b - m_c} (M_{\Lambda_c} - \bar{M}_D), \\ \lambda_1^B &= \lambda_1^M + \frac{2m_b m_c}{m_b - m_c} \left[(M_{\Lambda_b} - \bar{M}_B) - (M_{\Lambda_c} - \bar{M}_D) \right], \\ \bar{M}_B &= \frac{M_B + 3M_{B^*}}{4}, \quad \bar{M}_D = \frac{M_D + 3M_{D^*}}{4}.\end{aligned}\tag{7}$$

In Eq. (7), $\bar{\Lambda}^B$ and λ_1^B are the parameters for baryons and $\bar{\Lambda}^M$ and λ_1^M those for mesons. Later on, we will go back to the usual notation without attaching superscripts explicitly.

To form the bounds, one just takes the proper moments of the structure functions according to the combination required in the sum rules given in Section III. To this order, the Λ_{QCD}/m_Q corrections will depend on two HQET parameters; $\bar{\Lambda}$, λ_1 . As mentioned above, we take their values from the mesonic ones, where a certain linear relation has been determined [13]. We will use three different parameter sets to show the dependence on $\bar{\Lambda}$ and λ_1 : (A) $\bar{\Lambda} = 0.74$ GeV and $\lambda_1 = -0.43$ GeV 2 , (B) $\bar{\Lambda} = 0.64$ GeV and $\lambda_1 = -0.33$ GeV 2 , (C) $\bar{\Lambda} = 0.84$ GeV and $\lambda_1 = -0.53$ GeV 2 .

The sum rule for bounding $(\omega - 1) |F_1(\omega)|^2 / (2\omega)$ uses T_1 with vector-vector currents. The upper bound is simply the zeroth moment of T_1 , which is by Eq. (2)

$$\frac{(\omega - 1)}{2\omega} |F_1(\omega)|^2 \leq I_1^{(0)VV} + A_1^{(0)VV}.\tag{8}$$

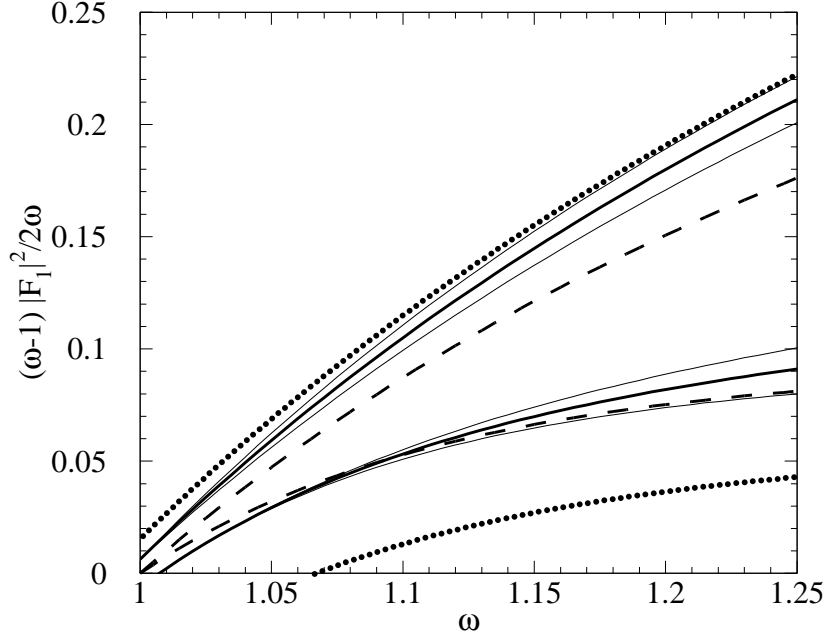


FIG. 1. *Upper and lower bounds on $(\omega - 1) |F_1(\omega)|^2 / (2\omega)$. The thick solid (dotted) curves are the upper and lower bounds including perturbative corrections for HQET parameter set (A) described in the text, and $\Delta = 1$ GeV (2 GeV). The dashed curves are the bounds without perturbative corrections, also for HQET parameter set (A). The thin solid curves show the dependence on $\bar{\Lambda}$ and λ_1 , using parameter sets (B) and (C), with $\Delta = 1$ GeV. Here the outer two thin solid curves are from parameter set (B), while the inner two curves from set (C)*

The first moment of T_1 is needed for the lower bound, which is

$$\frac{(\omega - 1)}{2\omega} |F_1(\omega)|^2 \geq I_1^{(0)VV} + A_1^{(0)VV} - \frac{1}{E_{\Lambda_1} - E_{\Lambda_c}} (I_1^{(1)VV} + A_1^{(1)VV}) \quad (9)$$

The upper and lower bounds are shown in Fig. 1.² For this section, the dotted curves are the bounds without perturbative corrections using set (A) above, while the solid and dashed curves represent the bounds including the perturbative corrections with $\Delta = 1$ GeV and $\Delta = 2$ GeV, respectively. We have shown the bounds in the kinematic range $1 \leq \omega \lesssim 1.25$,

²For all the figures in this section we take $m_b = 4.8$ GeV, $m_c = 1.4$ GeV, $\alpha_s = 0.3$ (corresponding to a scale of about 2 GeV). The values of $\bar{\Lambda}$ and λ_1 are discussed in the text.

where the higher order correction $\alpha_s(\omega - 1)^2$ should be negligible. The thin solid curves use the other HQET parameter sets (B) and (C).

In Fig. 1, the bounds without perturbative corrections approach zero because of the overall factor $\omega - 1$ appearing in the nonperturbative corrections. As we move the scale of Δ from 1GeV to 2GeV, the upper bound is only shifted upward by about 0.01, while the lower bound is dragged down by more than 0.04. This serves as an indication that in general perturbative corrections have a larger influence on the lower bound. The bounds get wider at small momentum transfer with parameter set (B) while narrower with set (C). As a general tendency in this and subsequent plots, varying among the three parameter sets (A), (B), and (C) usually makes less change on the upper bound than the lower bound. Here, the variations on the upper and lower bounds at $\omega = 1$ are about 5% and 11%, respectively.

A similar set of bounds for $(\omega + 1) |G_1(\omega)|^2 / 2\omega$ can be obtained by simply changing VV (vector-vector currents) to AA (axial-axial currents) in the above formulae.³ The bounds in this case are shown in Fig. 2. Perturbative corrections drag the bounds lower. From the bounds corresponding to $\Delta = 2\text{GeV}$ we also observe that the lower bound has been significantly decreased. In this case, the parameter set (B) lowers the bounding curves, but set (C) pushes them up. The variations of the upper and lower bounds at $\omega = 1$ by these parameter changes are about 1.5% and 17%, respectively.

The bounds on the other form factors involve higher moments of T_4 and T_5 . The upper bound for $(\omega^2 - 1) |F_2(\omega) - F_3(\omega)|^2 / 2\omega$ is, from Eq. (5),

$$\begin{aligned} F_{23}^{upper} = (\omega - 1) \left\{ & \frac{2}{\omega - 1} I_1^{(0)VV} + I_2^{(0)VV} + I_4^{(2)VV} - 2(M_{\Lambda_b} + M_{\Lambda_c}) I_4^{(1)VV} \right. \\ & + (M_{\Lambda_b} + M_{\Lambda_c})^2 I_4^{(0)VV} - 2I_5^{(1)VV} + 2(M_{\Lambda_b} + M_{\Lambda_c}) I_5^{(0)VV} \\ & + \frac{2}{\omega - 1} A_1^{(0)VV} + A_2^{(0)VV} + A_4^{(2)VV} - 2(M_{\Lambda_b} + M_{\Lambda_c}) A_4^{(1)VV} \\ & \left. + (M_{\Lambda_b} + M_{\Lambda_c})^2 A_4^{(0)VV} - 2A_5^{(1)VV} + 2(M_{\Lambda_b} + M_{\Lambda_c}) A_5^{(0)VV} \right\}. \end{aligned} \quad (10)$$

The lower bound is $(\omega^2 - 1) |F_2(\omega) - F_3(\omega)|^2 / 2\omega \geq F_{23}^{lower}$, with

³This set of bounds has been mentioned in [9], and we agree with their results.

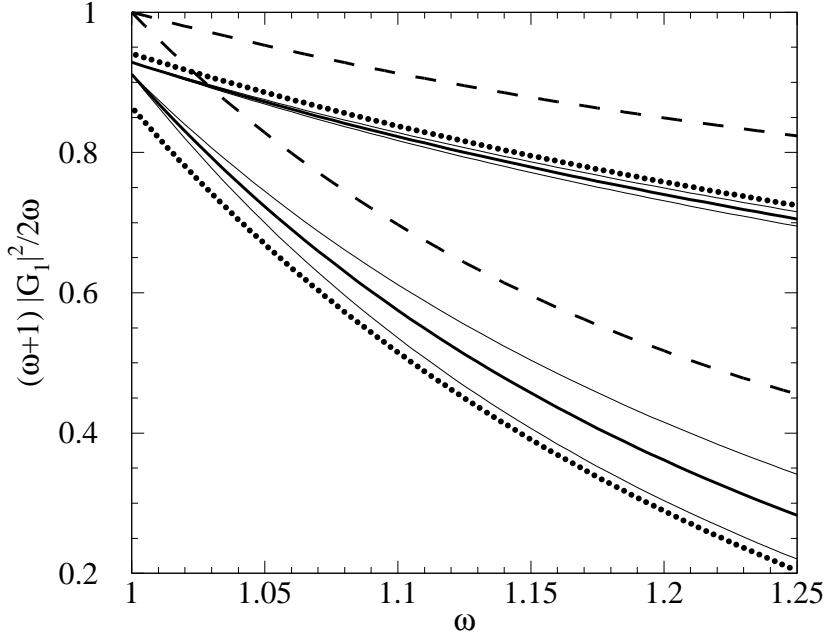


FIG. 2. *Upper and lower bounds on $(\omega + 1) |G_1(\omega)|^2 / (2\omega)$. The curves are labeled the same as in Fig. 1. Here the parameter set (B) gives the lower set of thin solid curves while the set (C) gives the upper set of curves.*

$$\begin{aligned}
F_{23}^{lower} &= F_{23}^{upper} & (11) \\
&- \frac{(\omega - 1)}{M_{\Lambda_1} - M_{\Lambda_c}} \left\{ \frac{2}{\omega - 1} I_1^{(1)VV} + I_2^{(1)VV} + I_4^{(3)VV} - 2(M_{\Lambda_b} + M_{\Lambda_c}) I_4^{(2)VV} \right. \\
&+ (M_{\Lambda_b} + M_{\Lambda_c})^2 I_4^{(1)VV} - 2I_5^{(2)VV} + 2(M_{\Lambda_b} + M_{\Lambda_c}) I_5^{(1)VV} \\
&\left. - \frac{2}{\omega - 1} A_1^{(1)VV} + A_2^{(1)VV} + A_4^{(3)VV} - 2(M_{\Lambda_b} + M_{\Lambda_c}) A_4^{(2)VV} \right. \\
&\left. + (M_{\Lambda_b} + M_{\Lambda_c})^2 A_4^{(1)VV} - 2A_5^{(2)VV} + 2(M_{\Lambda_b} + M_{\Lambda_c}) A_5^{(1)VV} \right\}.
\end{aligned}$$

They are plotted in Fig. 3. Notice that at tree level both bounds are identically zero. This can be easily understood from the relations in Eq. (4), $|F_2 - F_3|^2 \sim \bar{\Lambda}^2/m_Q^2$. Nevertheless, perturbative physics separates the bounds by pushing the upper bound higher to around 0.01 over the entire kinematic range while drawing the lower bound negative. Since the factors we are bounding are all positive definite, the lower bound is still zero. Changing Δ from

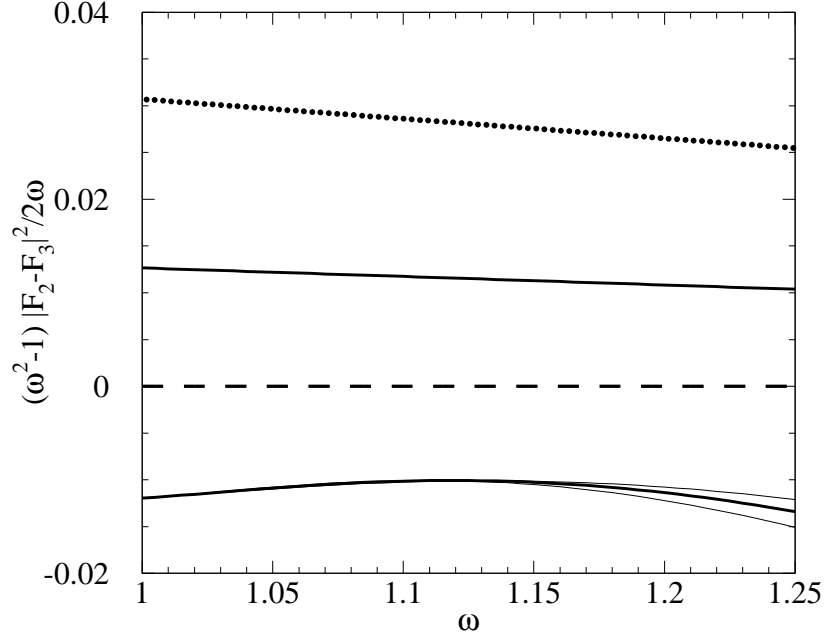


FIG. 3. *Upper and lower bounds on $(\omega^2 - 1) |F_2(\omega) - F_3(\omega)|^2 / 2\omega$. The curves are labeled the same as in Fig. 1.*

1 GeV to 2 GeV loosens the upper bound by more than a factor of two. Parameter sets (A), (B), and (C) have no influence on the upper bound because $\bar{\Lambda}$ and λ_1 only enter the upper bound through the tree-level corrections and they vanish to the order under consideration.

The upper bound for $(\omega - 1) |G_2(\omega) + G_3(\omega)|^2 / 2\omega$ is, from Eq. (6),

$$\begin{aligned}
G_{23}^{upper} = & -\frac{2}{\omega + 1} I_1^{(0)AA} + I_2^{(0)AA} + I_4^{(2)AA} - 2(M_{\Lambda_b} - M_{\Lambda_c}) I_4^{(1)AA} \\
& + (M_{\Lambda_b} - M_{\Lambda_c})^2 I_4^{(0)AA} - 2I_5^{(1)AA} + 2(M_{\Lambda_b} - M_{\Lambda_c}) I_5^{(0)AA} \\
& + \frac{2}{\omega - 1} A_1^{(0)AA} + A_2^{(0)AA} + A_4^{(2)AA} - 2(M_{\Lambda_b} - M_{\Lambda_c}) A_4^{(1)AA} \\
& + (M_{\Lambda_b} - M_{\Lambda_c})^2 A_4^{(0)AA} - 2A_5^{(1)AA} + 2(M_{\Lambda_b} - M_{\Lambda_c}) A_5^{(0)AA}.
\end{aligned} \tag{12}$$

The lower bound is $(\omega - 1) |G_2(\omega) + G_3(\omega)|^2 / 2\omega \geq G_{23}^{lower}$, with

$$\begin{aligned}
G_{23}^{lower} = & G_{23}^{upper} \\
& - \frac{1}{M_{\Lambda_1} - M_{\Lambda_c}} \left\{ -\frac{2}{\omega + 1} I_1^{(1)AA} + I_2^{(1)AA} + I_4^{(3)AA} - 2(M_{\Lambda_b} - M_{\Lambda_c}) I_4^{(2)AA} \right.
\end{aligned} \tag{13}$$

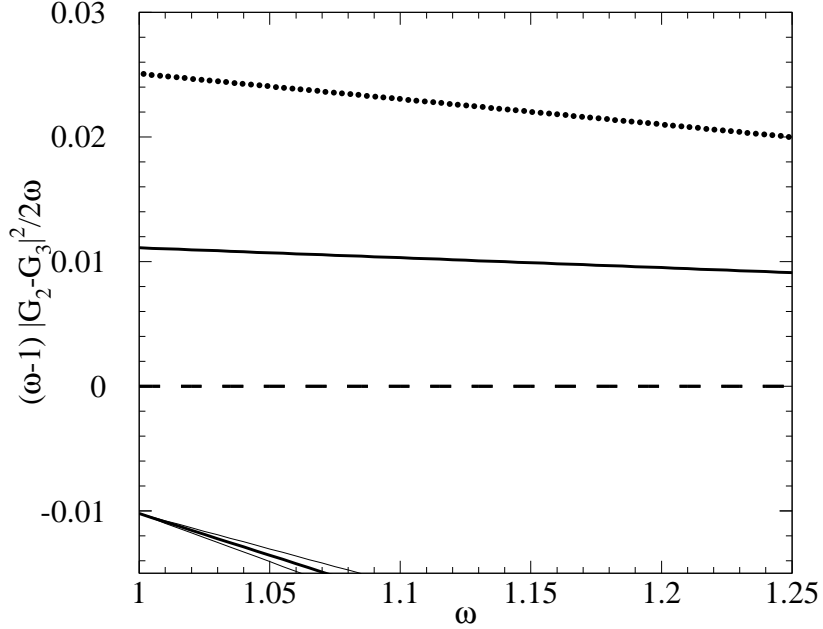


FIG. 4. *Upper and lower bounds on $(\omega - 1) |G_2(\omega) + G_3(\omega)|^2 / 2\omega$. The curves are labeled the same as in Fig. 1.*

$$\begin{aligned}
& + (M_{\Lambda_b} - M_{\Lambda_c})^2 I_4^{(1)AA} - 2I_5^{(2)AA} + 2(M_{\Lambda_b} - M_{\Lambda_c})I_5^{(1)AA} \\
& - \frac{2}{\omega + 1} A_1^{(1)AA} + A_2^{(1)AA} + A_4^{(3)AA} - 2(M_{\Lambda_b} - M_{\Lambda_c})A_4^{(2)AA} \\
& + (M_{\Lambda_b} - M_{\Lambda_c})^2 A_4^{(1)AA} - 2A_5^{(2)AA} + 2(M_{\Lambda_b} - M_{\Lambda_c})A_5^{(1)AA} \}.
\end{aligned}$$

The bounds on this form factor are shown in Fig. 4. Again, for the same reason as in the previous case, both the upper and lower bounds at tree level are identically zero, and the upper bound does not split for different parameter sets. The perturbative corrections also push both bounds in the current case away from zero; and using $\Delta = 2$ GeV in the calculation widens the upper bound by more than a factor of 2.

At $\mathcal{O}(\Lambda_{\text{QCD}}/m_Q)$, the upper bounds will not depend upon λ_1 . However, since $1/(M_{D1} - M_D) \sim 1/\Lambda_{\text{QCD}}$ its value will affect the lower bounds. It is possible to obtain the upper bounds to order $\mathcal{O}(\Lambda_{\text{QCD}}^2/m_Q^2)$, since at this order there are no new parameters in the OPE.

These corrections only slightly modify the upper bounds in Figs. 1 and 2 but greatly loosen the ones in Figs. 3 and 4 to around 0.1 over the entire kinematic range.

V. COMPARISON WITH MODELS

We choose from the literature the following commonly used form factor models for comparison with our bounds:

- (1) Soliton Model [14],
- (2) MIT Bag Model [15],
- (3) BS Model [16],
- (4) Relativistic 3-Quark Model [17],
- (5) COQM Model [18].

The soliton model [14] considers baryons with a single heavy quark c (or b) in the large N_c limit as bound states of D and D^* mesons (or B and B^* mesons) with baryons containing only light u and d quarks, which can be viewed as solitons in this limit. The MIT Bag Model used in [15] is actually a modified one that takes into account the familiar picture from the nonrelativistic quark model that treats the light component of a baryon as a diquark. The Relativistic 3-Quark Model [17] modifies the interaction Lagrangian between heavy hadrons and quarks by incorporating the spin structure imposed by the spectator quark model. Finally, the COQM model [18] uses the covariant quark model. All these models give Isgur-Wise functions without a dependence on the heavy quark masses. Thus, we use Eqs. (4) to relate the form factors to this Isgur-Wise function.

Figs. 5-8 show the different form factors from the models and the bounding curves. In plotting these figures, we used $m_b = 4.8$ GeV, $m_c = 1.4$ GeV, $\alpha_s = 0.3$ (corresponding to a scale of about 2 GeV), $\Delta = 1$ GeV and current PDG data on heavy meson masses. As mentioned above, λ_1 and $\bar{\Lambda}$ are not easy to obtain experimentally. Here we pick the parameter set (A) discussed above, $\bar{\Lambda} = 0.74$ GeV, $\lambda_1 = -0.43$ GeV². The uncertainty on λ_1 and $\bar{\Lambda}$ will correspondingly slightly modify our bounds, as discussed before.

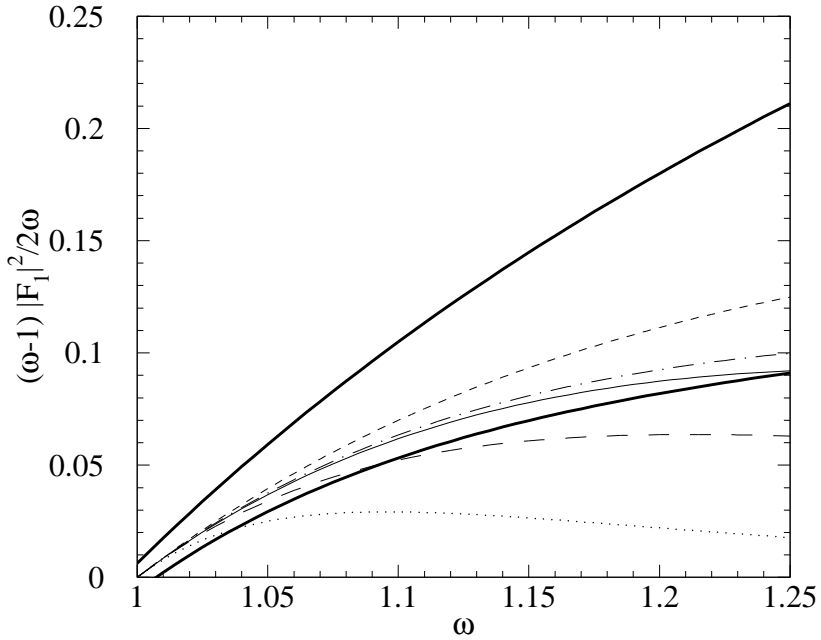


FIG. 5. The model values of $(\omega - 1) |F_1(\omega)|^2 / (2\omega)$ along with the corresponding bounds for comparison. The thick solid lines are the upper and lower bounds. The thin solid curve is the Soliton Model. The long dashed curve is the MIT Model, and the short dashed curve is the BS Model. The dot-dashed curve is the Relativistic 3-Quark Model. The dotted curve is the COQM Model.

Fig. 5 shows the model values of $(\omega - 1) |F_1(\omega)|^2 / (2\omega)$ along with the corresponding bounds for comparison. The Soliton Model, Relativistic 3-Quark Model and the BS Model agree with our bounds over the entire kinematic regime. The MIT Bag Model only slightly violates the lower bound, whereas the COQM model falls far below the lower bound at large recoil. If a larger Δ value is employed, all the model curves would fit into the bounds as one can check from Fig. 1.

The curves for $(\omega + 1) |G_1|^2 / 2\omega$ are shown in Fig. 6. All models start from one at zero recoil. This is because they do not incorporate the perturbative renormalization effect. The COQM Model quickly becomes too small in the large recoil regime. This, along with Fig. 5, tells us that the contribution from $\Lambda_b \rightarrow \Lambda_c$ at small momentum transfer is underestimated in the COQM Model. The other models are consistent with our bounds at large recoil and,

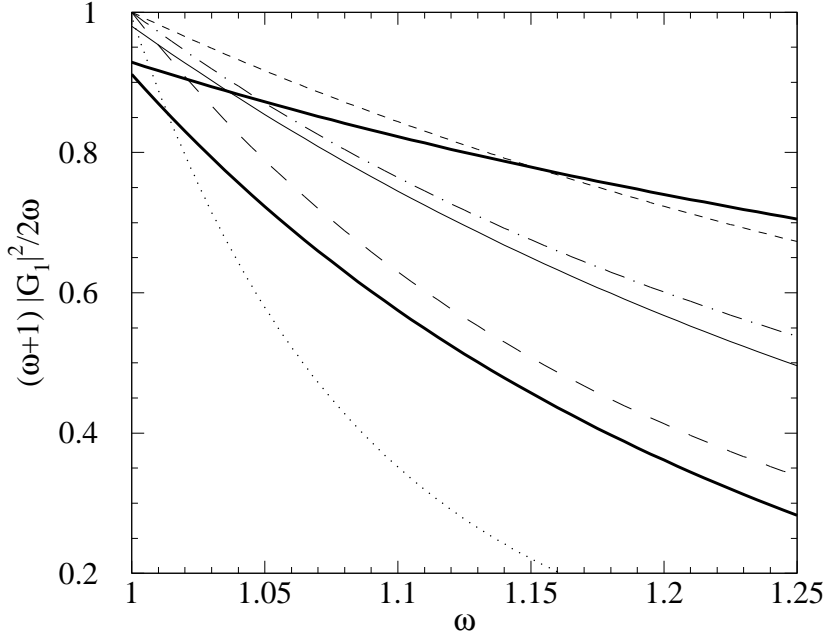


FIG. 6. The model values of $(\omega + 1) |G_1|^2 / 2\omega$ along with the corresponding bounds for comparison. The curves are labeled the same as in Fig. 5.

presumably, will nicely fit into our bounds near zero recoil if renormalization corrections are included.

Fig. 7 and Fig. 8 show that all the model predictions are well within our bounds for $(\omega^2 - 1) |F_2 - F_3|^2 / (2\omega)$ and $(\omega - 1) |G_2 + G_3|^2 / 2\omega$, respectively.

The scale we chose for these plots was $\Delta = 1$ GeV, since this gives tighter bounds. Had we chosen 2 GeV as our working scale, the bounds would be less stringent and thus would accommodate the models which originally fell slightly outside our bounds.

VI. ORDER $\alpha_s^2 \beta_0$ CORRECTIONS AT ZERO RECOIL

As in the case of heavy mesons, one can perform analogous numerical calculation to get the $\alpha_s^2 \beta_0$ contribution to structure functions and the bounds at zero recoil [19,20]. The results for the zeroth and first moments of the structure functions are presented in Table 1

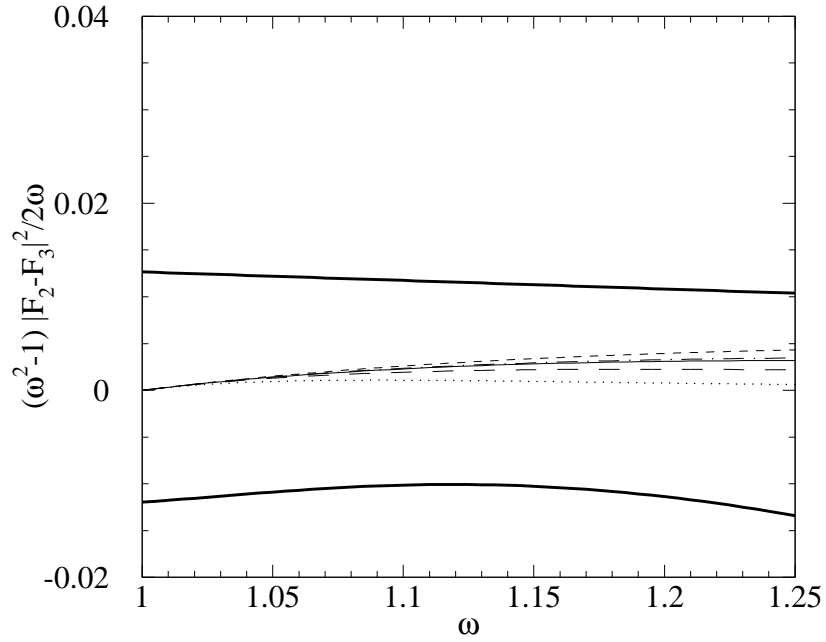


FIG. 7. The model values of $(\omega^2 - 1) |F_2 - F_3|^2 / (2\omega)$ along with the corresponding bounds for comparison. The curves are labeled the same as in Fig. 5.

of [5], for $\Delta = 1, 2$ GeV.

The $O(\alpha_s^2 \beta_0)$ corrections to the upper and lower bounds on the form factors at zero recoil are shown in Table 1 for $\Delta = 1$ GeV. In this case, the $O(\alpha_s^2 \beta_0)$ corrections are seen to be rather small, which gives us confidence that the perturbative expansion for the bounds is under control.

VII. BOUNDS ON SEMILEPTONIC DECAY SPECTRUM AND ITS SLOPE

The differential decay rate of $\Lambda_b \rightarrow \Lambda_c l \nu$ is

$$\frac{d\Gamma(\Lambda_b \rightarrow \Lambda_c l \nu)}{d\omega} = \frac{G_F^2}{24\pi^3} |V_{cb}|^2 m_{\Lambda_b}^5 z^3 \sqrt{\omega^2 - 1} F(z, \omega)^2, \quad (14)$$

where

$$F(z, \omega)^2 = (\omega - 1) |(z + 1)F_1 + (\omega + 1)(zF_2 + F_3)|^2 \quad (15)$$

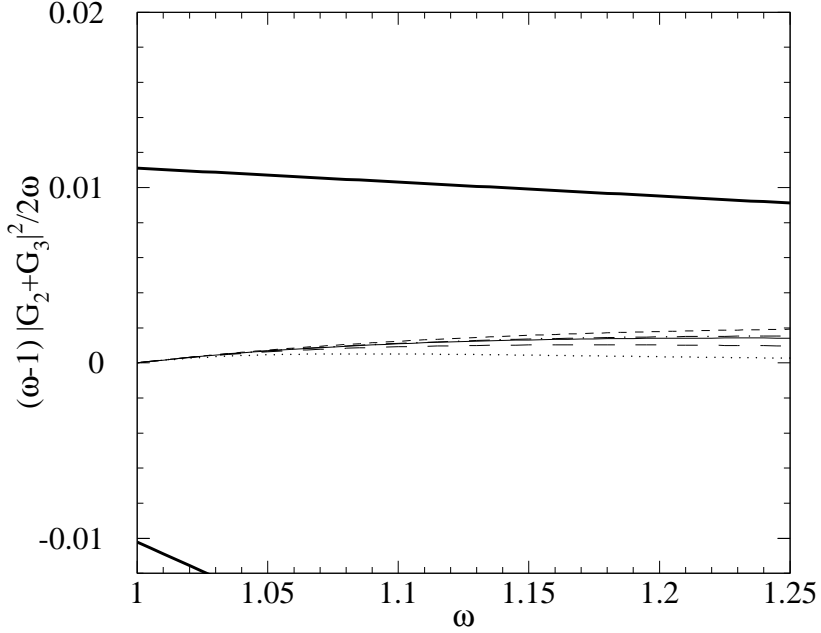


FIG. 8. The model values of $(\omega - 1) |G_2 + G_3|^2 / 2\omega$ along with the corresponding bounds for comparison. The curves are labeled the same as in Fig. 5.

$$\begin{aligned}
& + (\omega + 1) |(z + 1)G_1 + (\omega - 1)(zG_2 + G_3)|^2 \\
& + 2(z^2 - 2\omega z + 1) [(\omega - 1)|F_1|^2 + (\omega + 1)|G_1|^2].
\end{aligned}$$

In the linear approximation in $\omega - 1$, $F(z, \omega)^2$ can be expanded to be

$$F(z, \omega)^2 = F(z, 1)^2 \left[1 - \rho_{\Lambda_b}^2(\omega - 1) + \dots \right], \quad (16)$$

where $\rho_{\Lambda_b}^2$ is the slope of the spectrum at zero recoil. The combination of structure functions used to bound $F(z, \omega)^2$ is

$$\begin{aligned}
T(\epsilon) = 2\omega & \left[3(z^2 - 2\omega z + 1)(T_1^{VV} + T_1^{AA}) + 2(\omega z - 1) \epsilon (T_1^{VV} + T_1^{AA}) \right. \\
& \left. + \epsilon^2 (T_1^{VV} + T_1^{AA}) + z^2(w^2 - 1)(T_2^{VV} + T_2^{AA}) \right].
\end{aligned} \quad (17)$$

The bounds are drawn in Fig. 9. Here we use the decay rate spectrum over the full kinematic range to extract the bounds for the slope. As seen from the bounded region in the plot, the

	Tree Level	$O(\alpha_s)$	$O(\alpha_s^2 \beta_0)$
Upper $\frac{\omega-1}{2\omega} F_1 ^2$	0	0.0063	0.0042
Lower $\frac{\omega-1}{2\omega} F_1 ^2$	0	-0.0060	-0.0028
Upper $\frac{\omega^2-1}{2\omega} F_2 - F_3 ^2$	0	0.0127	0.0083
Lower $\frac{\omega^2-1}{2\omega} F_2 - F_3 ^2$	0	-0.0119	-0.0056
Upper $\frac{\omega+1}{2\omega} G_1 ^2$	1	-0.0713	0.0159
Lower $\frac{\omega+1}{2\omega} G_1 ^2$	1	-0.0885	0.0031
Upper $\frac{\omega-1}{2\omega} G_2 + G_3 ^2$	0	0.0111	0.0071
Lower $\frac{\omega-1}{2\omega} G_2 + G_3 ^2$	0	-0.0102	-0.0026

TABLE I. Bound on form factors at zero recoil, evaluated with $\Delta = 1$ GeV.

allowed range of the slope is $0.87 < \rho_{\Lambda_b}^2 < 4.82$. This agrees with the lattice calculation [21] of $\rho_{\Lambda_b}^2 = 2.4 \pm 4$.

VIII. DISCUSSION

Many of the general features of our bounds had been mentioned in our previous work [5]. In the specific application of these bounds to heavy baryons, we find that they provide more stringent conditions on the leading form factors, F_1 and G_1 . Looser bounds hold for “subleading” form factors that are suppressed by $1/M_Q$ in magnitude, namely, $|F_2 - F_3|$ and $|G_2 + G_3|$. Our bounds typically have much better predictive power near maximal momentum transfer. However, they are not stringent enough in the above mentioned “subleading” form factors. This is because both the form factors are too small and the whole factor is suppressed by $\omega-1$. However, perturbative corrections do not give vanishing contributions to the bounds at zero recoil. The bounds also become less stringent as Δ increases. Therefore, we should use the smallest value of Δ for which the perturbative expansion still works.

We also observed that the $O(\alpha_s^2 \beta_0)$ corrections to the bounds at zero recoil are small for $\Delta = 1$ GeV. This in turn suggests that a perturbative expansion in this problem works

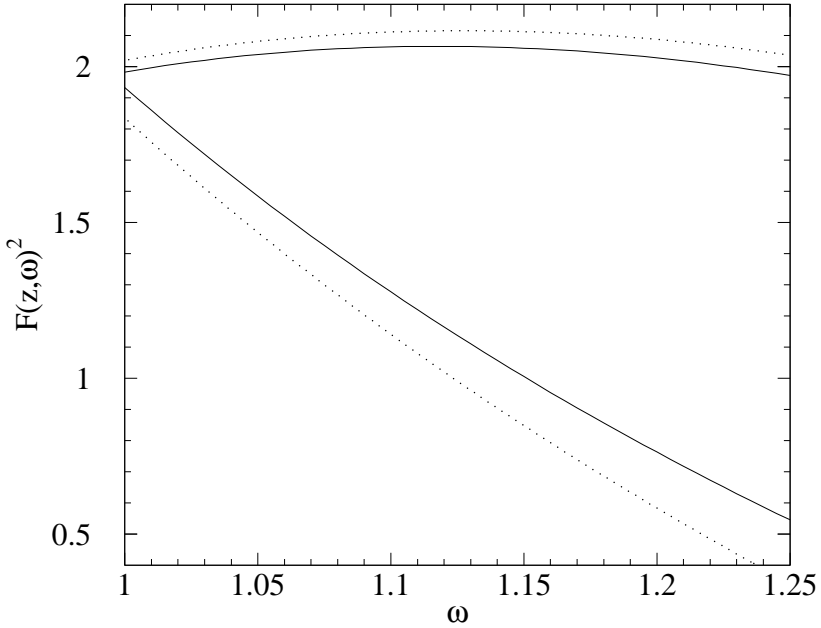


FIG. 9. *Upper and lower bounds on $F(z, \omega)^2$. The solid (dotted) curves are the upper and lower bounds including perturbative corrections for HQET parameter set (A) described in the text, and $\Delta = 1$ GeV (2 GeV).*

well at this scale, provided that the $O(\alpha_s^2 \beta_0)$ corrections dominate in the complete $O(\alpha_s^2)$ corrections. (Typically $O(\alpha_s^2 \beta_0)$ accounts for about 90% of the complete $O(\alpha_s^2)$ corrections.)

We show the bounds for the differential decay rate of $\Lambda_b \rightarrow \Lambda_c l \nu$ and give bounds on its slope, $0.87 < \rho_{\Lambda_b}^2 < 4.82$. None of the models quoted here take into account the renormalization corrections, and therefore they fail specific bounds, such as the one in Fig. 7, as $\omega \rightarrow 1$. In particular, this will affect the extraction of the Kobayashi-Maskawa matrix element $|V_{cb}|$ from the zero recoil limit of the semileptonic decay spectrum. Also, this will give an incorrect estimate on the experimental backgrounds and efficiencies. Therefore, the models should be properly modified accordingly to have more sensible form factors.

ACKNOWLEDGMENTS

I would like to thank Adam Leibovich in particular for discussions and help on various technical issues. It is also a pleasure to thank Fred Gilman and Ira Rothstein for valuable suggestions. This work was supported in part by the Department of Energy under Grant No. DE-FG02-91ER40682.

REFERENCES

- [1] M. Neubert, Phys. Lett. **B264**, 455-461 (1991).
- [2] CDF Collaboration, Phys. Rev. Lett. **77**, 1439-1443 (1996).
- [3] OPAL Collaboration, Z. Phys. **C74**, 423-435 (1997).
- [4] C.G. Boyd and R.F. Lebed, Nucl. Phys. **B485**, 275-290 (1997).
- [5] C-W. Chiang and A.K. Leibovich, hep-ph/9906420 (1999).
- [6] N. Isgur and M.B. Wise, Phys. Lett. **B348**, 276-292 (1991).
- [7] I. Bigi, M. Shifman, N.G. Uraltsev, and A. Vainshtein, Phys. Rev. **D52**, 196-235 (1995).
- [8] C.G. Boyd and I.Z. Rothstein, Phys. Lett. **B395**, 96-106 (1997); Phys. Lett. **B420**, 350-358 (1998).
- [9] C.G. Boyd, Z. Ligeti, I.Z. Rothstein, and M.B. Wise, Phys Rev. **D55**, 3027-3037 (1997).
- [10] H. Georgi, B. Grinstein, and M.B. Wise, Phys. Lett. **B252**, 456-460 (1990).
- [11] A.F. Falk and M. Neubert, Phys. Rev. **D47**, 2982-2990 (1993).
- [12] A.V. Manohar and M.B. Wise, Phys. Rev. **D49**, 1310-1329 (1994).
- [13] M. Gremm, A. Kapustin, Z. Ligeti, and M.B. Wise, Phys. Rev. Lett. **77**, 20-23 (1996).
- [14] E. Jenkins, A.V. Manohar, and M.B. Wise, Nucl. Phys. **B396**, 27-37 (1993); E. Jenkins, A.V. Manohar, and M.B. Wise, *ibid.* **B396**, 38-52 (1993).
- [15] M. Sadzikowski and K. Zalewski, Z. Phys. **C59**, 677-681 (1993).
- [16] M.A. Ivanov, J.G. Körner, V.E. Lyubovitskij, and A.G.Rusetsky, Phys. Rev. **D59**, 074016 (1999).
- [17] M.A. Ivanov, J.G. Körner, V.E. Lyubovitskij, and A.G.Rusetsky, Phys. Rev. **D57**, 5632-5652 (1998).
- [18] R. Mohanta, A.K. Giri, M.P. Khana, M. Ishida, S. Ishida, and M. Oda, Prog. Theor. Phys. **4**, 101 (1999).
- [19] B.H. Smith and M.B. Voloshin, Phys. Lett. **B340**, 176-180 (1994).
- [20] A. Kapustin, Z. Ligeti, M.B. Wise, and B. Grinstein, Phys. Lett. **B375**, 327-334 (1996).
- [21] UKQCD Collaboration, Nucl. Phys. Proc. Suppl. **53**, 408-412 (1997).